Cell Reports, Volume *33*

Supplemental Information

Respiratory Supercomplexes Promote Mitochondrial Efficiency and Growth in Severely Hypoxic Pancreatic Cancer

Kate E.R. Hollinshead, Seth J. Parker, Vinay V. Eapen, Joel Encarnacion-Rosado, Albert Sohn, Tugba Oncu, Michael Cammer, Joseph D. Mancias, and Alec C. Kimmelman

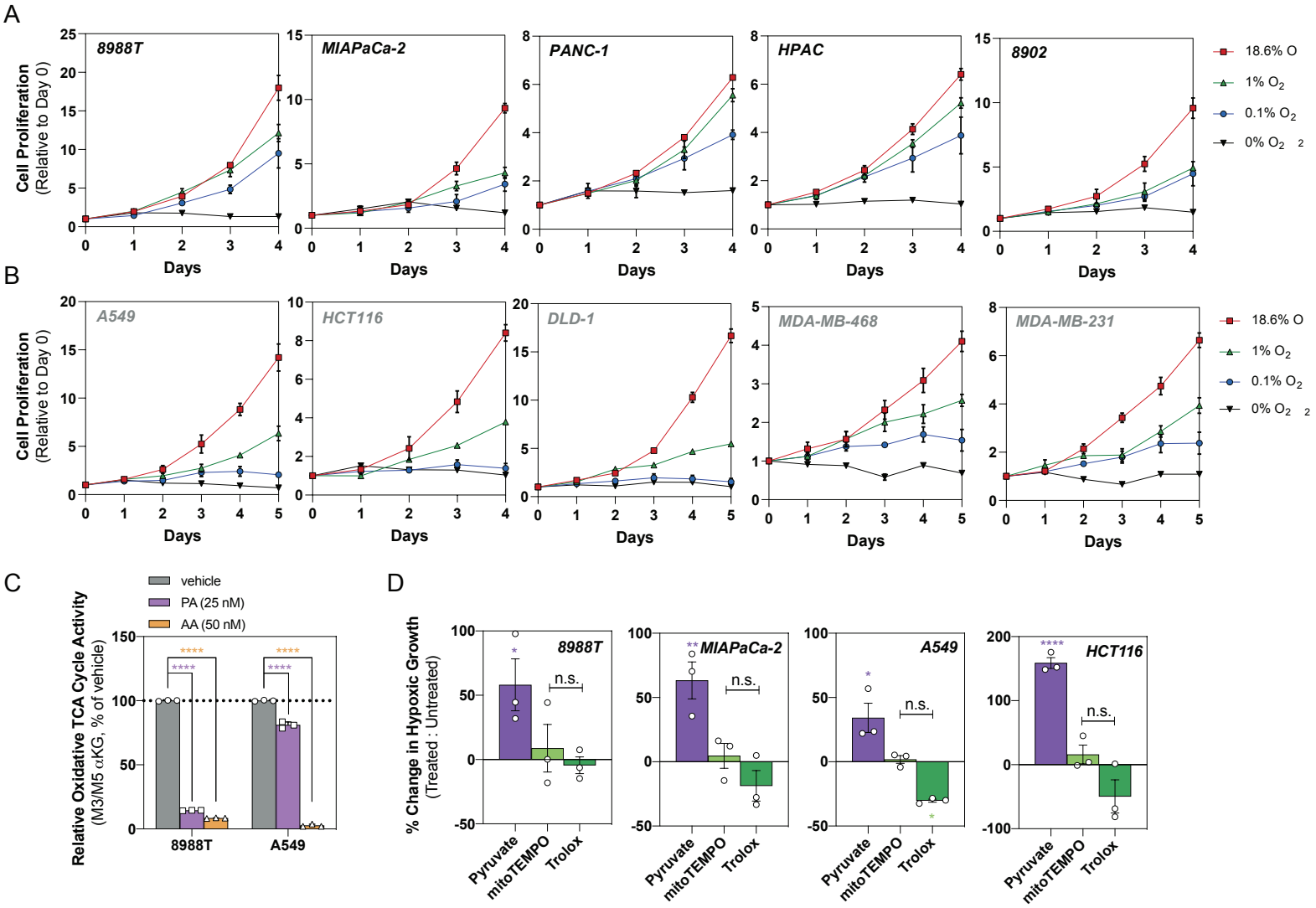

Figure S1 – Growth characteristics of cancer cell lines in hypoxia, related to Figure 1.
(A) Relative growth of pancreatic cancer cells 8988T, MIAPaCa-2, PANC-1, HPAC and 8902 exposed to normoxia (18.6% O_2), hypoxia (1% O_2), severe hypoxia (0.1% O_2), or anoxia (0% O_2). Data normalized to day 0 (mean ± SEM, n=3).
(B) Relative growth of lung cancer cell line A549, colon cancer cell lines HCT116 and DLD-1, and breast cancer cell lines MDA-MB-468 and MDA-MB-231 exposed to normoxia (18.6% O_2), hypoxia (1% O_2), severe hypoxia (0.1% O_2), or anoxia (0% O_2). Data normalized to day 0 (mean ± SEM, n=3).
(C) Relative oxidative TCA cycle activity determined by calculating the ratio of M+3 : M+5 α-ketoglutarate from [U]-$^{13}C_5$-glutamine in 8988T and A549 cells upon addition of piericidin A (25 nM) and antimycin A (50 nM) for 24 h. Data is shown as a percentage of vehicle (mean ± SD, n=3).
(D) Percent change in hypoxic growth in 8988T, MIAPaCa-2, A549 and HCT116 cells on addition of pyruvate (1 mM), mitoTEMPO (20 μM) and Trolox (5 mM) for 5 days in severe hypoxia (0.1% O_2). Data shown as a percentage of vehicle (mean ± SEM, n=3).
Significance determined using Dunnett's multiple comparisons test in S1C-D, where n.s. >0.05, * 0.05>p, ** 0.01>p, **** p≤0.0001.

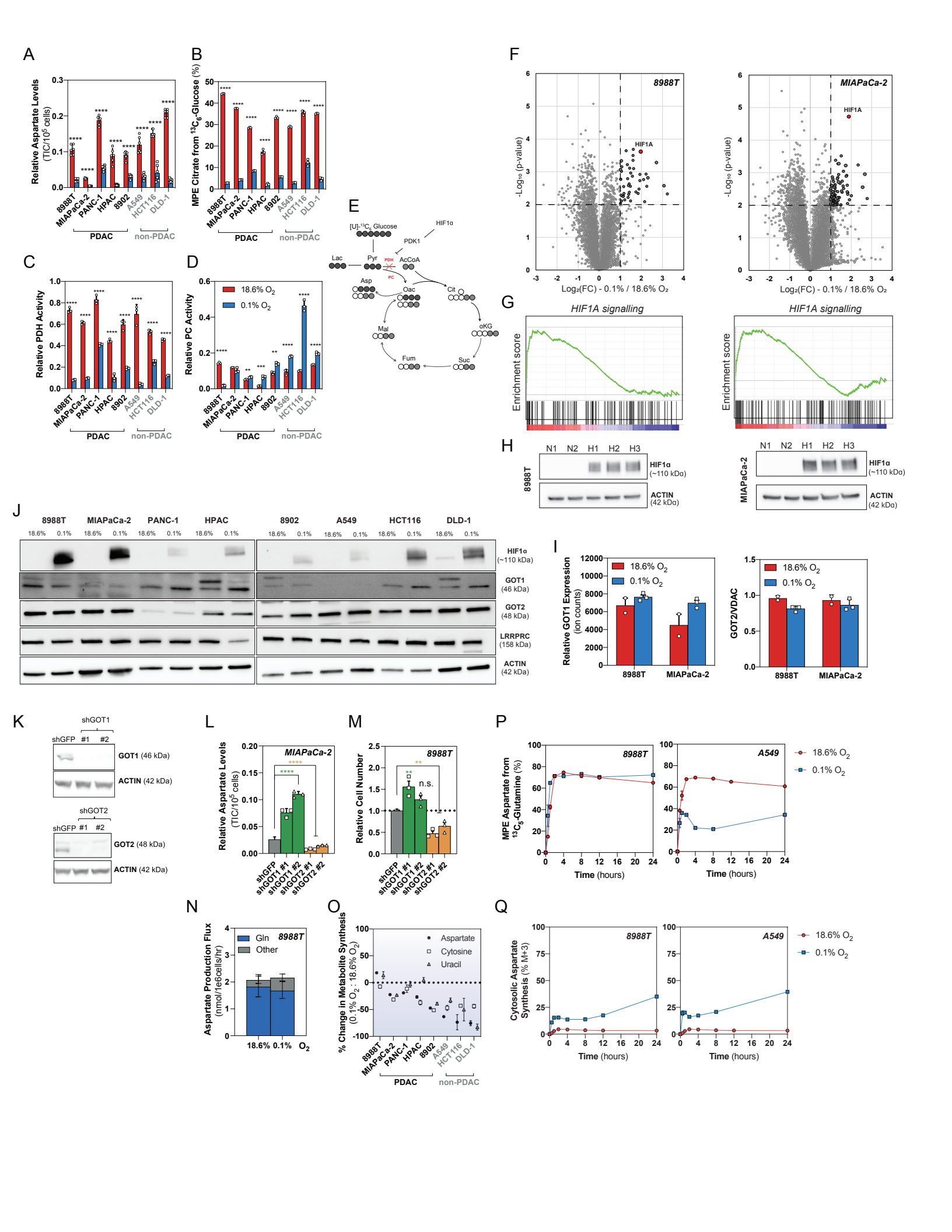
A
Relative Aspartate Levels (TIC/10^5 cells)
8988T
MIAPaCa-2
PANC-1
HPAC
8902
A549
HCT116
DLD-1
PDAC
non-PDAC
B
MPE Citrate from 13C6-Glucose (%)
C
Relative PDH Activity
D
Relative PC Activity
18.6% O2
0.1% O2
E
[U]-13C6 Glucose
HIF1α
PDK1
Lac
Pyr
PDH
AcCoA
PC
Asp
Oac
Cit
Mal
αKG
Fum
Suc
F
8988T
MIAPaCa-2
HIF1A
-Log10 (p-value)
Log2(FC) - 0.1% / 18.6% O2
G
HIF1A signalling
Enrichment score
H
N1 N2 H1 H2 H3
HIF1α (~110 kDa)
ACTIN (42 kDa)
J
HIF1α (~110 kDa)
GOT1 (46 kDa)
GOT2 (48 kDa)
LRRPRC (158 kDa)
ACTIN (42 kDa)
I
Relative GOT1 Expression (ion counts)
GOT2/VDAC
K
shGOT1
shGFP #1 #2
GOT1 (46 kDa)
ACTIN (42 kDa)
shGOT2
GOT2 (48 kDa)
L
Relative Aspartate Levels (TIC/10^5 cells)
shGFP
shGOT1 #1
shGOT1 #2
shGOT2 #1
shGOT2 #2
M
Relative Cell Number
n.s.
P
MPE Aspartate from 13C5-Glutamine (%)
Time (hours)
N
Aspartate Production Flux (nmol/1e6cells/hr)
Gln
Other
18.6% 0.1% O2
O
% Change in Metabolite Synthesis (0.1% O2 : 18.6% O2)
Aspartate
Cytosine
Uracil
Q
Cytosolic Aspartate Synthesis (% M+3)

Figure S2 – Pancreatic cancer cells decrease glucose oxidation but maintain oxidative glutamine metabolism during severe hypoxia, related to Figure 2.

(A) Relative aspartate levels, across cell lines exposed to 24 h severe hypoxia (0.1% O_2), where total ion counts (TIC) are normalized to extraction efficiency and cell number (mean ± SD, n=3). Significance determined using an unpaired, two-tailed Student's t-test, where **** p<0.0001.

(B) Mole percent enrichment (MPE) of citrate from [U]-$^{13}C_6$-glucose across cell lines exposed to 24 h severe hypoxia (0.1% O_2) (mean ± SD, n=3). Significance determined using an unpaired, two-tailed Student's t-test where **** p<0.0001.

(C) Relative PDH activity after 24 h severe hypoxia (0.1% O_2) determined by calculating the ratio of M+2 aspartate : M+3 pyruvate (mean ± SD, n=3). Significance determined using an unpaired, two-tailed Student's t-test, where **** p<0.0001.

(D) Relative PC activity after 24 h in severe hypoxia (0.1% O_2) determined by calculating the ratio of M+3 aspartate : M+3 pyruvate (mean ± SD, n=3). Significance determined using an unpaired, two-tailed Student's t-test, where n.s. >0.05, ** 0.01>p, *** 0.001>p, **** p<0.0001.

(E) Schematic diagram to show downstream label incorporation from [U]-$^{13}C_6$ glucose. M+2 aspartate is produced through the activity of pyruvate dehydrogenase (PDH) and M+3 aspartate is produced through the activity of pyruvate carboxylase (PC).

(F) Volcano plot of differentially expressed proteins in 8988T (left) and MIAPaCa-2 (right) pancreatic cancer cell lines between normoxia and severe hypoxia (0.1% O_2). Proteins were considered differentially changed if they had a Log2 fold change (FC) of >1 or <-1 and an adjusted p-value <0.05. HIF1α is upregulated ~2-fold in both datasets, with a p-value of 0.0002 and 0.00002 for 8988T and MIAPaCa-2 cells, respectively.

(G) Gene set enrichment analysis (GSEA) of 8988T (left) and MIAPaCa-2 (right) demonstrating increased HIF1α signaling when cells are exposed to severe hypoxia (0.1% O_2). Significant changes in upregulated proteins include those involved in the canonical HIF1α signaling pathway.

(H) Representative western blot of 8988T (left) and MIAPaCa-2 (right) cell samples used in the proteomics screen confirming increased HIF1α expression in hypoxic samples. Two replicates were used for normoxic samples (N1, and N2) and three replicates were used for hypoxic samples (H1, H2, and H3).

(I) Relative expression in 8988T and MIAPaCa-2 cells quantified by summing reporter ion counts of peptide-spectral matches for GOT1 (left) and GOT2 (right). GOT2 expression is normalized to the mitochondrial marker VDAC.

(J) Representative western blot of HIF1α, GOT1/2, LRRPRC and ACTIN expression in cell line panel exposed to 24 h of normoxia or severe hypoxia (0.1% O_2).

(K) Representative western blot demonstrating loss of GOT1 (top) and GOT2 (bottom) using two independent hairpins in MIAPaCa-2 cells.

(L) Relative aspartate levels in MIAPaCa-2 cells with loss of GOT1 or GOT2 after 24 h in severe hypoxia (0.1% O_2), where total ion counts (TIC) are normalized to extraction efficiency and cell number (mean ± SD, n=3). Significance determined using Dunnett's multiple comparison test, where **** p<0.0001.

(M) Relative growth in 8988T cells with loss of either GOT1 or GOT2 after 5 days growth in severe hypoxia (0.1% O_2) (mean + SEM, n=3). Significance determined using Dunnett's multiple comparison test, where n.s. >0.05, ** 0.01>p.

(N) Aspartate production flux from [U]-$^{13}C_5$-glutamine and unlabeled sources (other) in normoxia and severe hypoxia (0.1% O_2) (mean ± 95% CI, n=3).

(O) Percent change in ^{13}C incorporation in severe hypoxia (0.1% O_2) compared to normoxia for metabolites aspartate, cytosine, and uracil from [U]-$^{13}C_5$-glutamine (mean ± SD, n=3).

(P) Moles percent enrichment (MPE) of aspartate from [U]-$^{13}C_5$-glutamine in 8988T (left) and A549 (right) cells in normoxia and severe hypoxia severe hypoxia (0.1% O_2) (mean ± SD, n=3).

(Q) Kinetic labeling data in cytosolic aspartate production (M+3) in normoxic and severely hypoxia (0.1% O_2) 8988T (left) and A549 (right) cells using [U]-$^{13}C_5$-glutamine (mean ± SD, n=3).

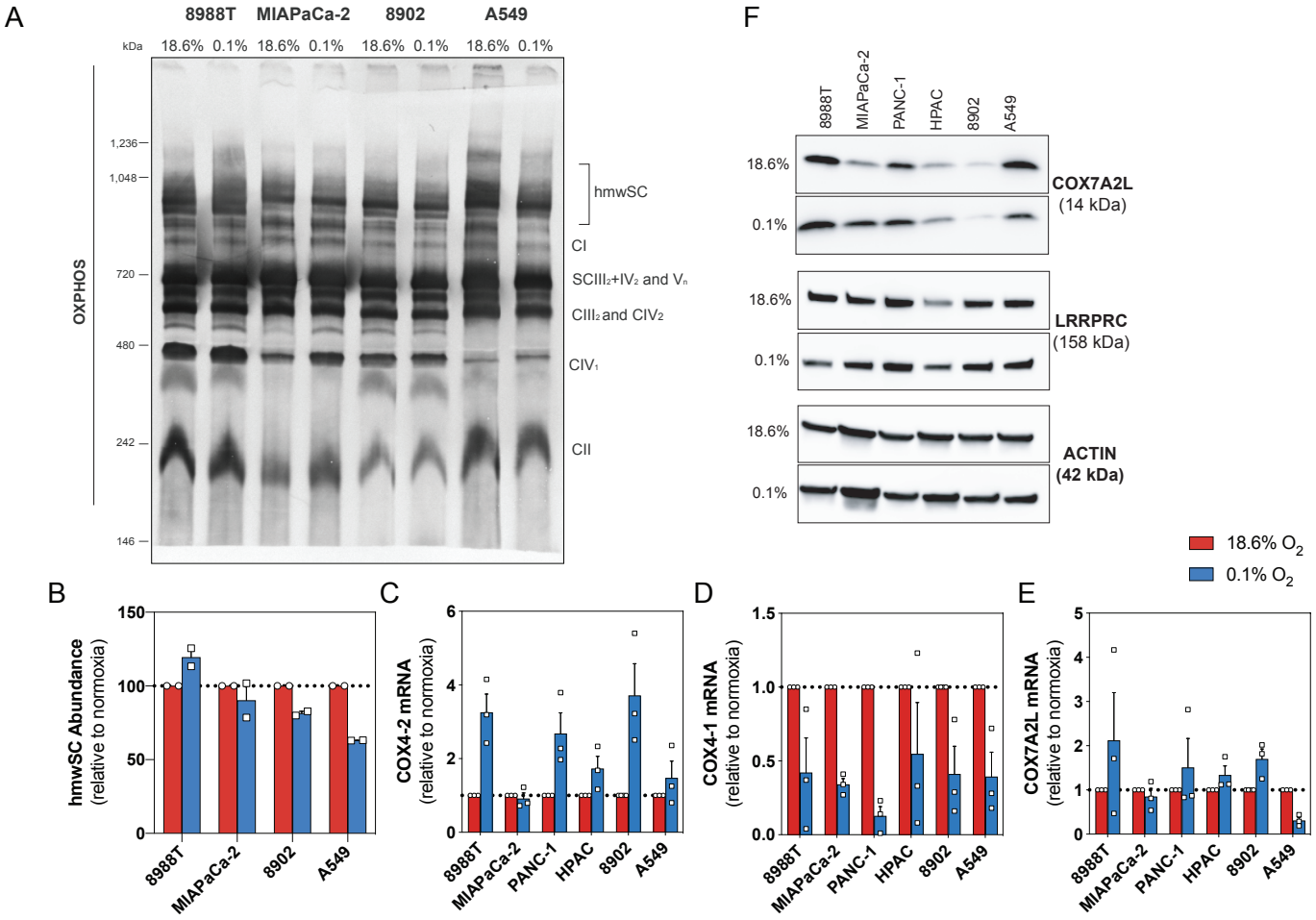

Figure S3 – Pancreatic cancer cells maintain mitochondrial supercomplex abundance and COX7A2L expression in severe hypoxia, related to Figure 3.

(A) Representative BN-PAGE demonstrating respiratory supercomplex abundance and composition in 8988T, MIAPaCa-2, 8902 and A549 cells exposed to normoxia or 24 h severe hypoxia (0.1% O_2) by immunoblotting with an OXPHOS antibody against NDUFB8, SDHB, UQCR2, MTCO1 and ATP5a. Samples normalized to cell number and mitochondrial content.

(B) Quantification of high molecular weight supercomplexes (hmwSC) in 8988T, MIAPaCa-2, 8902 and A549 cells exposed to normoxia or 24 h severe hypoxia (0.1% O_2). Data is shown relative to normoxic control (mean ± SEM, n=2).

(C) Relative increase in mRNA expression of COX4-2 in a panel of cancer cell lines exposed to 24 h of severe hypoxia (0.1% O_2) (mean ± SEM, n=3).

(D) Relative decrease in mRNA expression of COX4-1 in a panel of cancer cell lines exposed to 24 h of severe hypoxia (0.1% O_2) (mean ± SEM, n=3).

(E) Relative mRNA expression of COX7A2L in a panel of cancer cell lines exposed to 24 h of severe hypoxia (0.1% O_2) (mean ± SEM, n=3).

(F) Representative western blot of COX7A2L, LRRPRC and ACTIN expression in cell line panel exposed to 24 h of normoxia or severe hypoxia (0.1% O_2).

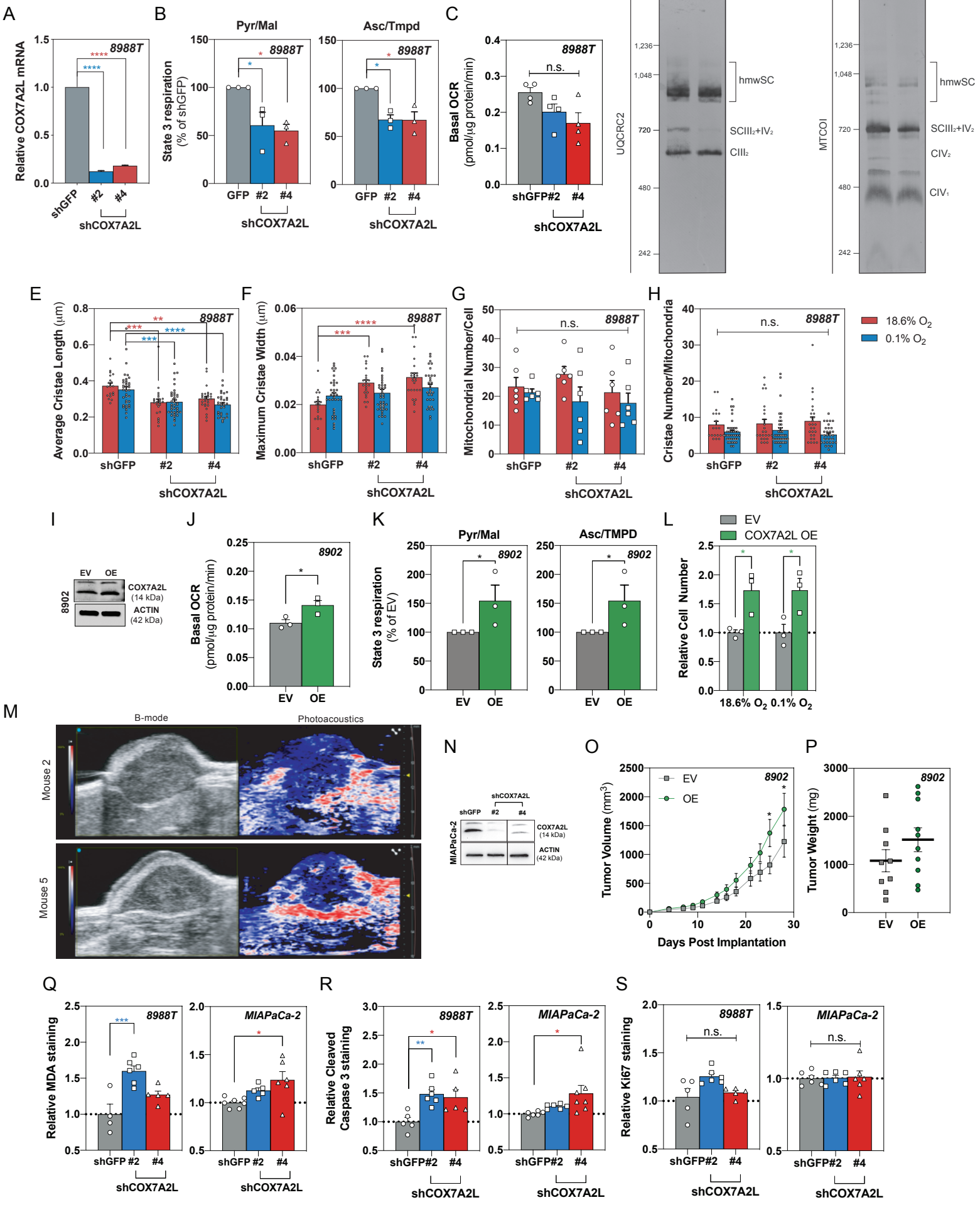
A
Relative COX7A2L mRNA
8988T
shGFP
#2
#4
shCOX7A2L
B
Pyr/Mal
Asc/Tmpd
State 3 respiration (% of shGFP)
8988T
GFP
#2
#4
shCOX7A2L
C
Basal OCR (pmol/μg protein/min)
8988T
n.s.
shGFP#2
#4
shCOX7A2L
D
shGFP
shCOX7A2L-2
kDa
1,236
1,048
720
480
242
UQCRC2
hmwSC
SCIII2+IV2
CIII2
MTCOI
hmwSC
SCIII2+IV2
CIV2
CIV1
E
Average Cristae Length (μm)
8988T
shGFP
#2
#4
shCOX7A2L
F
Maximum Cristae Width (μm)
8988T
shGFP
#2
#4
shCOX7A2L
G
Mitochondrial Number/Cell
n.s.
8988T
shGFP
#2
#4
shCOX7A2L
H
Cristae Number/Mitochondria
n.s.
8988T
18.6% O2
0.1% O2
shGFP
#2
#4
shCOX7A2L
I
EV
OE
8902
COX7A2L (14 kDa)
ACTIN (42 kDa)
J
Basal OCR (pmol/μg protein/min)
8902
EV
OE
K
Pyr/Mal
Asc/TMPD
State 3 respiration (% of EV)
8902
EV
OE
L
EV
COX7A2L OE
Relative Cell Number
18.6% O2
0.1% O2
M
B-mode
Photoacoustics
Mouse 2
Mouse 5
N
shCOX7A2L
shGFP
#2
#4
MIAPaCa-2
COX7A2L (14 kDa)
ACTIN (42 kDa)
O
EV
OE
8902
Tumor Volume (mm3)
Days Post Implantation
P
8902
Tumor Weight (mg)
EV
OE
Q
Relative MDA staining
8988T
MIAPaCa-2
shGFP
#2
#4
shCOX7A2L
R
Relative Cleaved Caspase 3 staining
8988T
MIAPaCa-2
shGFP#2
#4
shCOX7A2L
S
Relative Ki67 staining
8988T
MIAPaCa-2
n.s.
shGFP#2
#4
shCOX7A2L

Figure S4 – Loss of COX7A2L decreases expression and function of CIII and CIV containing supercomplexes, related to Figure 4.

(A) Representative Q-PCR demonstrating decreased COX7A2L expression in 8988T cells using two independent hairpins (mean ± SD, n=3).

(B) Oxygen consumption rate (OCR) of cells fed CI-linked oxidizable substrate pyruvate and malate (left) and CIV-linked oxidizable substrate ascorbate and N,N,N',N' Tetramethyl-p-phenylenediamine (TMPD) (right) in 8988T cells upon loss of COX7A2L. Basal OCR shown as a percentage of shGFP control (mean ± SEM, n=3).

(C) Basal OCR in 8988T cells upon loss of COX7A2L. Data shown as a percentage of shGFP control (mean ± SEM, n=4).

(D) Representative BN-PAGE demonstrating a decrease in CIII containing supercomplexes by immunoblotting with an antibody against UQCR2 (left) and a decrease in CIV containing supercomplexes by immunoblotting with an antibody against MTCO1 (right). Samples normalized to cell number and mitochondrial content.

(E) Average cristae length determined from 19-39 mitochondria in 8988T cells with loss of COX7A2L in normoxia and severe hypoxia (0.1% O_2) (mean ± SEM, n>18).

(F) Maximal cristae width determined from 19-39 mitochondria in 8988T cells with loss of COX7A2L in normoxia and severe hypoxia (0.1% O_2) (mean ± SEM, n>18).

(G) Quantification of mitochondrial number per cell in 8988T cells with loss of COX7A2L in normoxia and severe hypoxia (0.1% O_2). A minimum of six images were analyzed per condition at 3400x magnification in a user blinded fashion (mean ± SEM, n=6).

(H) Quantification of cristae number per mitochondria determined from 19-39 mitochondria in 8988T cells with loss of COX7A2L in normoxia and severe hypoxia (0.1% O_2) (mean ± SEM, n>18).

(I) Representative western blot demonstrating overexpression of COX7A2L in 8902 cells.

(J) Basal OCR in 8902 cells on overexpression of COX7A2L. Data shown as a percentage of shGFP control (mean ± SEM, n=3).

(K) Oxygen consumption rate (OCR) of cells fed CI-linked oxidizable substrate pyruvate and malate (left) and CIV-linked oxidizable substrate ascorbate and N,N,N',N' Tetramethyl-p-phenylenediamine (TMPD) (right) in 8902 cells on overexpression of COX7A2L. Basal OCR shown as a percentage of shGFP control (mean ± SEM, n=3).

(L) Relative cell number in 8902 cells on overexpression of COX7A2L after 4 days in normoxia and severe hypoxia (0.1% O_2).

(M) Photoacoustic imaging of subcutaneous models of pancreatic cancer three weeks post implantation. B-mode (left) provides anatomical details. Photoacoustic image (right) represents oxygen saturation where red indicates areas of high oxygenation and blue represents areas of low oxygenation.

(N) Representative western blot demonstrating loss of COX7A2L expression in MIAPaCa-2 cells using RNAi. Blot cropped to remove lane 4.

(O) Measurements to determine tumor volume were recorded to assess tumor growth after 2 x 10^6 8902 cells with COX7A2L overexpression were implanted subcutaneously (mean ± SEM, n>8).

(P) Tumor weight was measured at endpoint (mean ± SEM, n>8).

(Q) Quantification of MDA staining intensity in 8988T (left) and MIAPaCa-2 (right) tumors expressing control or knockdown of COX7A2L. A minimum of 5 tumor sections were quantified per condition (mean ± SEM, n>5).

(R) Quantification of staining intensity for cleaved caspase 3 in 8988T (left) and MIAPaCa-2 (right) tumors expressing control or knockdown of COX7A2L. A minimum of 5 tumor sections were quantified per condition (mean ± SEM, n>5).

(S) Quantification of staining intensity for Ki67 in 8988T (left) and MIAPaCa-2 (right) tumors expressing control or knockdown of COX7A2L. A minimum of 5 tumor sections were quantified per condition (mean ± SEM, n>5).

Significance determined using Dunnett's multiple comparisons test for 4A-C, E-H and Q-S, where n.s. $\geq$0.05, * 0.05>p, ** 0.01>p, *** 0.001>p, **** p<0.0001.

Significant determined using an unpaired student's two tailed test for 4J-L, where * 0.05>p.

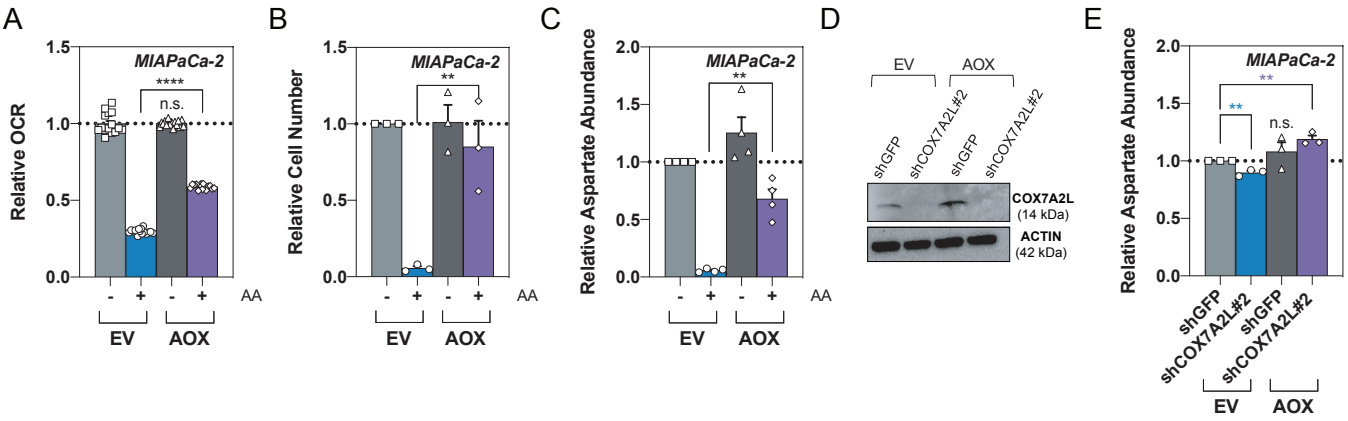

Figure S5 – Alternative oxidase (AOX) expression and function alleviates the metabolic defects caused by disrupting supercomplex assembly in hypoxia, related to Figure 5.

(A) Relative OCR in EV or AOX expressing MIAPaCa-2 cells on loss of COX7A2L in the presence of absence of 2 μM Antimycin A (mean ± SD, n=15).

(B) Relative cell number after 5 days proliferation in EV or AOX expressing MIAPaCa-2 on loss of COX7A2L in the presence of absence of 2 μM Antimycin A (mean ± SEM, n=3).

(C) Relative aspartate abundance in control or AOX expressing MIAPaCa-2 on loss of COX7A2L in the presence of absence of 2 μM Antimycin A (mean ± SEM, n=3).

(D) Representative western blot confirming loss of COX7A2L in MIAPaCa-2 expressing either control of AOX.

(E) Relative abundance of aspartate in control of AOX expressing MIAPaCa-2 cells on loss of COX7A2L in 1% O_2. Values are normalized to control after normalization to extraction efficiency and cell number (mean ± SEM, n=3).

Significance determined using an unpaired, two-tailed Student's t-test, where n.s. >0.05, * 0.05>p, ** 0.01>p, *** 0.001>p, **** p<0.0001.